

# Computational and Experimental Investigations on Thermal and Fluid Flow Characteristics for Different Models of Tapes Inserts with $\text{TiO}_2$ /Water Nanofluid under Turbulent Conditions

\* Fouad A. Saleh

Assist Prof., Mechanical Engineering Department, Al-Mustansiriyah University, Baghdad, Iraq.  
foads2003@yahoo.com

**Abstract-** Computational and experimental analysis aiming to recognizing the thermal and fluid flow physical behaviour of tubes fitted with different models of inserted tapes with using a distilled (pure) water and  $\text{TiO}_2$ /water nanofluid as working fluids for the turbulent Reynolds number range from 5,000 to 20,000 is carried out. The tubes with inserts showed better heat transfer rate when compared with plain tube. Nusselt number and friction factor become higher when using swirl generators inserts than their values in plain tapes inserts. Using of nanofluid with 0.1% nanoparticles volume fraction lead to enhance heat transfer rate with slightly increase in pressure drop and friction factor. The investigations included dual plain tapes, dual plain twisted tapes and dual helical screw twisted tapes inserts. The obtained results showed that, a maximum enhancement of 82.2% is achieved in the Nusselt number by using tube fitted with dual helical screw twisted tapes inserts and nanofluid than that observed with the plain tube and distilled water. And the maximum friction factor observed for the same model of the tube fitted with dual helical screw twisted tapes inserts and nanofluid are up to 17.34% than that of the plain tube.

**Index Term--** Multiple tapes inserts, multi-longitudinal vortices, nanofluid,  $\text{TiO}_2$ , heat transfer enhancement.

## 1. INTRODUCTION

The demand to improve heat exchange devices having a relatively small size is increasing due to their necessity in wide applications such as cooling system, domestic devices, electronic equipment, chemical process, etc. This has led to numerous heat transfer enhancement techniques. These techniques are tool for enhancing the rate of heat transfer process between fluid and boundary surface, also to reduce the spatial dimensions of system.

These techniques can be categorized to two main methods; (i) active method: which equip an additional power source for heat transfer improvement; (ii) passive method: use many modifications without any external power source such as additive surface (as spiral fin, helical screw twisted tapes,

twisted tapes, strips, etc), or by use of fluid additives as adding nanoparticles to the working fluid (nanofluid).

Nanofluid is a type of heat transfer fluid generated by mixing two phases materials where solid nanoparticles are dispersing in base fluid to form the nanofluid which has a different thermophysical properties than each one separately. Since the water (as a conventional fluid) has a relatively low quality of heat transfer behaviour, the nanofluids which formed by using water as conventional fluid open the door to obtained more benefits especially in heat transfer augment filed.

In the other hand, swirl flow generators such as (twisted tape, helical screw twisted tapes) has a thermal enhancement mechanism depend on produce secondary flow in form of vortex motion lead to mix fluid layers and reduce boundary layer thickness, that cause higher temperature gradient near the wall which lead to increase heat transfer rate.

The straight tapes (strips) also work as an enhancement inserts which causing a reduction in hydraulic diameter that corresponding to increase fluid velocity and heat transfer rate.

Behabadi [1], experimented the twisted tape insert in copper tube with R-134a flow, the inserts induced within flow core region, it is revealed that heat transfer coefficient and friction factor were higher than these obtained in plain tube. Subsequently, Bergles and Manglik [2], experimented the full length twisted tape insert with various twist ratios to illustrate the mechanism of heat transfer enhancement. Also empirical correlations were proposed to evaluate Nusselt number and friction factor.

Sunder and Sharma [3], reported experimentally the effect of twisted tape inserts in core flow of  $\text{Al}_2\text{O}_3$  nanofluid within a circular tube for different volume concentrations and thermal conditions on thermo-hydraulic characteristics. He [4], studied nanofluids behaviour concerning thermal characteristics in plain tube which given significant improvement in thermal performance with higher nanoparticles diameter and volume concentration.

Hu and Chang [5], conducted numerical simulation on the case of internal finned tube by straight tapes on boundary flow

heat transfer enhancement. Kelkar and Patankar [6], used an internal longitudinal strips within circular tube as internal fins where investigated for fluid flow and heat transfer rate characteristics.

Pourajabi [7], found that using of  $\text{Al}_2\text{O}_3$  /water nanofluid with twisted tape induced in core region reached a superior thermal performance with a noticeable increase in friction losses than water flow in plain tube. Said [8], reported the thermophysical properties of  $\text{Al}_2\text{O}_3$  and  $\text{TiO}_2$  nanoparticles with distilled water and proposed a parabolic equations for dynamic viscosity and thermal conductivity at specific conditions.

Maddah [9], investigated the using of nanofluid with single twisted tape insert in double pipe heat exchanger, it was achieved +20% and +2.5% percentage increment in overall heat transfer coefficient and friction factor, respectively, higher than that without insert.

Eiamsa-ard [10], presented experimentally the effect of nanofluid flow in tube fitted with multiple plain twisted tapes on Nusselt number and thermal performance factor. The results shown that Nusselt number and friction factors increased as the number of tapes and volumetric concentration increased.

Sandesh [11], presented an experimental study to evaluate thermal and hydraulic characteristics of helical screw inserts

(within core region) in  $\text{Al}_2\text{O}_3$ -water and carbon nano-tubes (CNT)-water nanofluids through a straight pipe in laminar flow regime.

As mentioned above and many other researches [12-16] which have studied thermal improvements, few studies were focused on inserts connected to tube wall with nanofluids effect on thermo-hydraulic characteristics. This study aiming to investigate, numerically and experimentally, the effect of three different dual models of inserted tapes connected to tube wall as an internal fins with  $\text{TiO}_2$ -Water nanofluid and with pure water on heat transfer rate and friction factor.

## 2. Inserts and Materials

### 2.1 Inserts

The geometries used in numerical and experimental analysis are made for tubes with dual strips (plain tapes), twisted tapes and helical screw twisted tapes inserted individually within the tube and welded symmetrically to tube wall.

The tube, as shown in Fig. (1), has a length (L) equal 1000mm and inner diameter (D) of 50mm.

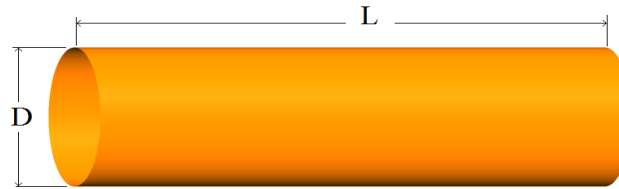


Fig. 1. Tube geometry.

Tube fitted with dual plain tapes (**TDPT**), tube fitted with dual plain twisted tapes (**TDPTT**) and tube fitted with dual helical screw twisted tapes (**TDHSTT**) are modelled and made. The schematic view of inlet cross sectional area of these geometries and parametric dimensions are showed and defined

in Fig. (2) and the 3D view of these models are viewed in Fig. (3).

The inserts induced through the whole length of test tube have a width (w), thickness ( $\delta$ ) and pitch of  $180^\circ$  twist ( $\gamma$ ) as defined in Table I.

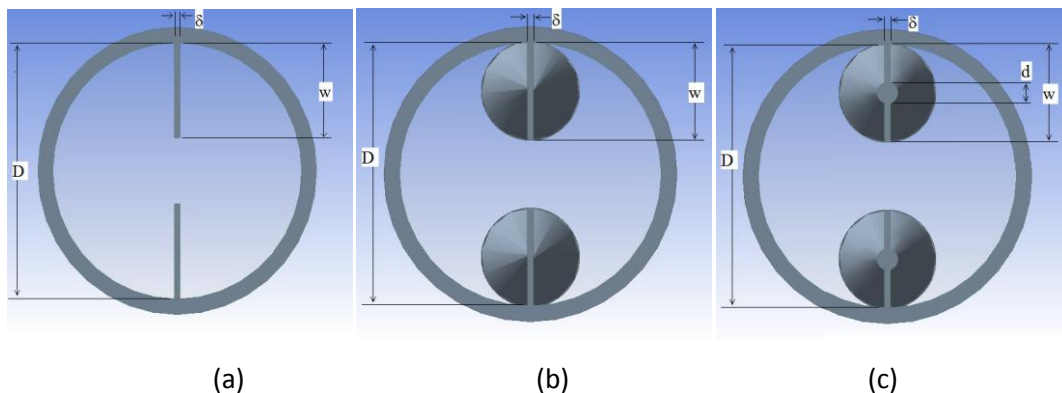


Fig. 2. Schematic view for tubes fitted with; (a) dual plain tapes, (b) dual plain twisted tapes, (c) dual helical screw twisted tapes.

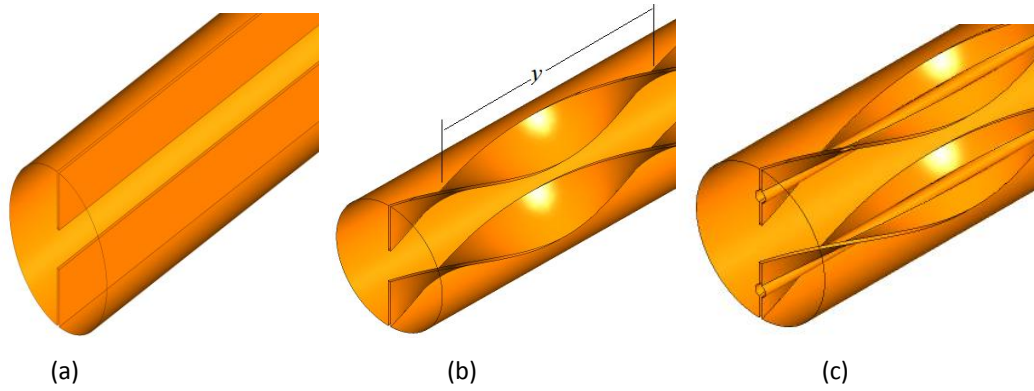


Fig. 3. Tubes fitted with different inserts; (a) TDPT, (b) TDPTT, (c) TDHSTT.

Table I  
Dimensions and details of inserts.

Model	No. of tapes	Tape width (mm)	Tape pitch (y) (mm)	Tape length (mm)	Tape thickness ( $\delta$ ) (mm)	Rod diameter (d) (mm)
TDPT	2	18.6	----	1000	1	----
TDPTT	2	18.6	100	1000	1	----
TDHSTT	2	18.6	100	1000	1	4

The *co-swirl* tape arrangement was considered for all models; all tapes were twisted in the same direction.

## 2.2 Working Fluids

Water was used in the prime tests to effort the effect of inserts only on the heat transfer and friction losses of tubes.

Eventually, nanofluid of TiO<sub>2</sub> nanoparticles pre-scattered in pure water used to evaluated the improvement rate by accompanying nanotechnology and the different models of inserts. In the current investigations, TiO<sub>2</sub> nanoparticles was equipped with a particles size of (<50nm) mixed with pure

water and stabilizers then sonicated continuously by ultrasonic vibrator generating pulses of 240W at  $40 \pm 4$  kHz to break nanoparticles agglomeration. Nanoparticles distribution was found to be stable during experiments period and no intermediate mixing process considered necessary. TiO<sub>2</sub> particles and water have the considered properties illustrated in table (2).

Table II  
Properties of titanium oxide particles [8] and water.

	Density ( $\rho$ ) kg/m <sup>3</sup>	Specific heat ( $C_p$ ) J/kg. K	Thermal conductivity(K) W/m.k	Dynamic viscosity( $\mu$ ) kg/m.s
TiO <sub>2</sub>	4230	692	8.4	----
Water	997.0089	4179	0.613	$855 \times 10^{-6}$

Nanoparticles volume concentration desired in this research was ( $\phi = 0.1\%$ ) for the TiO<sub>2</sub>/Water. The table (3) contains the popular and valid equations which used to evaluate thermophysical properties values of nanofluid and shows the values.

Table III  
Correlations of TiO<sub>2</sub>/Water properties and its values.

Property	Formula	Relation no.	Researcher	Value
Density ( $\rho$ )	$\rho_{nf} = \varphi\rho_{np} + (1 - \varphi)\rho_{bf}$	(1)	Pak[17]	1000.2419 kg/m <sup>3</sup>
Specific heat ( $C_p$ )	$(C_p)_{nf} = \varphi(C_p)_{np} + (1 - \varphi)(C_p)_{bf}$	(2)	[9]	4175.513 J/kg.K
Thermal conductivity(K)	$K_{nf} = [1 + 3\varphi]K_{bf}$	(3)	Effective medium theory [8]	0.61484 W/m.K
Dynamic viscosity( $\mu$ )	$\mu_{nf} = [1 + 2.5\varphi + 6.5\varphi^2]\mu_{bf}$	(4)	Batchelor[18]	857.143x10 <sup>-6</sup> kg/m.s

### 3. NUMERICAL MODELS

#### 3.1 Numerical Method and Simulation Conditions

The numerical analyses constructed on the steady and three dimensional continuity, momentum and energy equations.

it was performed by using the computational fluid dynamics ANSYS-Fluent commercial code. RNG  $k-\varepsilon$  turbulence model was selected to solve the considered computational domains because the effect of swirl on turbulence is included in this turbulence model which enhances the accuracy of swirling flows. Internal flow under external uniform heat flux condition considered for all domains as ( $\bar{q} = 30,000$  w/m<sup>2</sup>). The tube internal diameter denoted as  $D$ , and length  $L$  as explained previously.

No slip condition is also applied to the tube wall. Results are investigated only at fully developed region ( $L > 10D_h$ ).

At the inlet of the test tube, a velocity ( $V$ ) to give the required Reynolds number is specified by using the following correlation:

$$Re_{D_h} = \frac{v D_h}{\nu} \quad \dots (5)$$

Where ( $Re_{D_h}$ ) is the Reynolds number based on hydraulic diameter, ( $\nu$ ) is the kinematic viscosity of the working fluid and ( $D_h$ ) is the hydraulic diameter. **Water and TiO<sub>2</sub>/Water** are simulated as the working fluids and calculations for the thermophysical properties are taken at the inlet temperature of

300k which are explained in tables (2) for water and table (3) for nanofluid previously. The nanofluid considered as a single phase fluid with different physical parameters as density, thermal capability, thermal conductivity and viscosity than the conventional base fluid. Turbulent flow regime with a range for Reynolds number of (5,000-20,000) was studied.

The reference values were set at the inlet region. The hydraulic diameter at each inlet and outlet has the same value. At the outlet, a pressure outlet condition is selected and the gauge pressure is set to zero. And the turbulence intensity obtained from the expression

$$I = 0.16Re_{D_h}^{-0.125} \quad \dots (6)$$

Other flow quantities are extrapolated from the interior domain by the solver in ANSYS-Fluent software. The SIMPLE (Semi-Implicit Pressure Linked Equations) algorithm were chosen as solver method.

In addition, a convergence criterion of  $10^{-5}$  was used for energy, momentum and mass conservation of the calculated parameters.

#### 3.2 Grid Resolution

The tetrahedral volume mesh are used for representing the computational domains to set aside blurred curved volumes which couldn't be clearly simulated by hexahedral meshes, as shown in Fig. (4).

Grid systems with about (3,000,000) elements were utilized to the domains for the calculations.

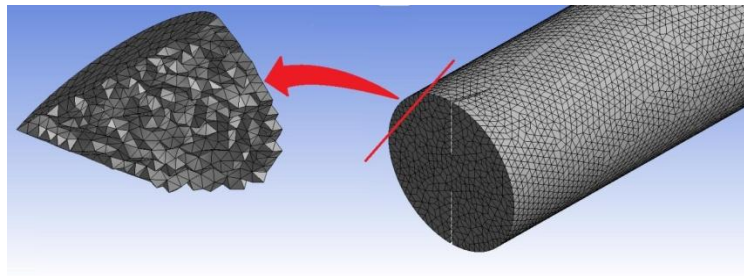


Fig. 4. Tetrahedral mesh cells with small cutted elements region.

#### 4. EXPERIMENTAL APPARATUS

The tests to investigate heat transfer rate and frictional losses were carried out by equipping the experimental set-up shown in Fig. (5).

It mainly consist of; a *steel test tube* of (1000mm) length with inner and outer diameters of (50mm) and (53mm) respectively. A *nichrome wire heater* wrapped over the outer surface of test tube with 5kW capacity. By a *glass-wool insulation*, both test tube and electrical heater are insulated from undesirable

surrounded heat transfer process. A *thermocouples* mentioned as (T1-9) in Fig. (5) tooled up to specify fluid temperature at inlet and both wall and fluid temperatures at fully developed and outlet regions, all of the thermocouples were calibrated before fixing them, and all were connected to the temperature reader (data logger) to measure temperature values.

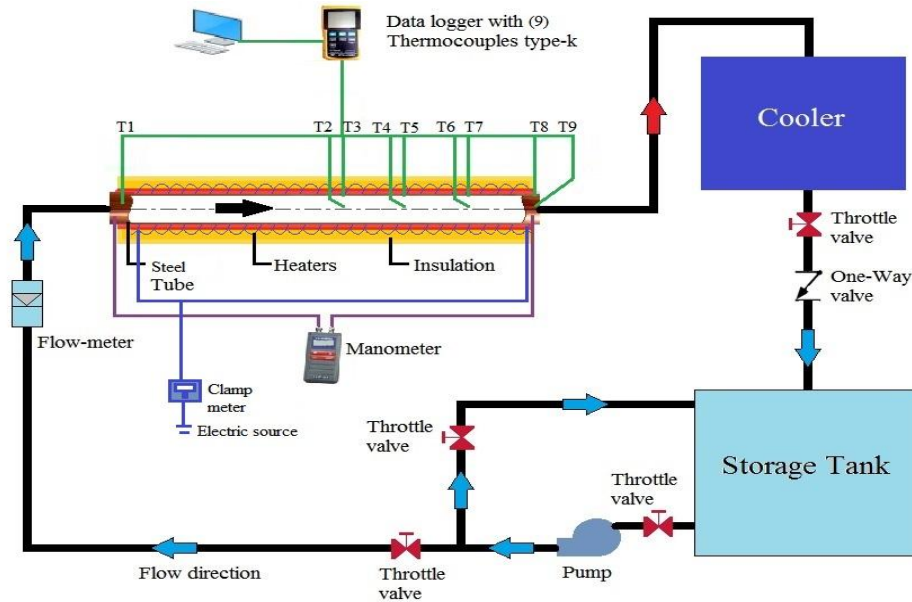


Fig. 5. Schematic diagram of the experimental setup.

A digital *manometer* used to specify pressure drop value along test section. By act of electrical heater, the working fluid temperature increased within the test section due to the uniform heat flux, then allowed to cool by passing through *cooler* (evaporative cooling system). By flow cycle, the working fluid return to the *storage tank* and then pumped again to the test section. *Flow-meter* was placed before the test section inlet in order to measure working fluids flow rate and determines the Reynolds number range.

To control fluid flow rate, a set of throttle valves are used for that purpose. Also for maintenance and emergency.

To ensure steady state condition for each test run, a delay period of (30) minutes was taken prior to the data record. The methodology of calculations used to evaluate heat transfer and fluid flow parameters for the experimental results are presented in section (5).

#### 5. CALCULATIONS

Nusselt number which represent the concept of heat transfer enhancement was estimated from the famous correlation;

$$Nu = \frac{h \cdot D_h}{K} = \frac{[\bar{q}/(T_s - T_b)] D_h}{K} \quad \dots (7)$$

For experimental tests, ( $T_s$ ) and ( $T_b$ ) was defined by the equations (8) and (9);

$$T_s = \frac{T_3 + T_5 + T_7 + T_9}{4} \quad \dots (8)$$

$$T_b = \frac{T_2 + T_4 + T_6 + T_8}{4} \quad \dots (9)$$

The uniform heat flux measured by expression;

$$\bar{q} = \frac{\text{Current} \times \text{Voltage}}{\pi DL} \quad \dots (9)$$

Current (Amps) and voltage (Volts) both re measured by using the clamp meter which illustrated in fig. (5)

Nusselt numbers values were validated with the empirical correlations from previous researches explained in table (4)

Table IV  
Correlations of Nusselt number validations.

Formula	Relation no.	Researcher	Remark
$Nu = \frac{\left(\frac{f}{8}\right) (Re_{Dh} - 1000) Pr}{1 + 12.7 \left(\frac{f}{8}\right)^{\frac{1}{2}} (Pr^{\frac{2}{3}} - 1)}$	(11)	Gnielinski [19]	plain tube with water flow
$Nu = 0.074 Re_{nf}^{0.707} Pr_{nf}^{0.385} \phi^{0.074}$	(12)	Duangthongsuk and Wongwises [9]	plain tube with nanofluid

The fanning friction factor is defined from Darcy-Weisbach equation for water and nanofluid flowing [20]:

$$f = \frac{\Delta p}{0.5 \rho V_{in}^2 \left(\frac{L}{D_h}\right)} \quad \dots (13)$$

Friction values were validated with the theoretical and empirical relations of other researchers for the basic cases that used plain tube without any additional surfaces and they were extrapolated in table (5)

Table V  
Correlations of friction factor validations.

Formula	Relation no.	Researcher	Remark
$f = 0.318 Re_{Dh}^{-0.25}$	(14)	Blasius [21]	plain tube with water flow
$f = (0.79 \ln Re_{Dh} - 1.64)^{-2}$	(15)	Petukhov [21]	plain tube with water flow
$f = 0.961 \phi^{0.052} Re_{Dh}^{-0.375}$	(16)	Duangthongsuk and Wongwises [9]	plain tube with nanofluid flow

Validation correlations in tables (4 & 5) were used for both numerical and experimental investigated results.

## 6. RESULTS AND DISCUSSIONS

### 6.1 Flow Structure

#### 6.1.1 Velocity Field

Fields of predicted velocity for numerical models in case of water flows are shown in Fig. (6). The contours are taken for  $Re=5,000$  and at various axial locations at the fully developed region.

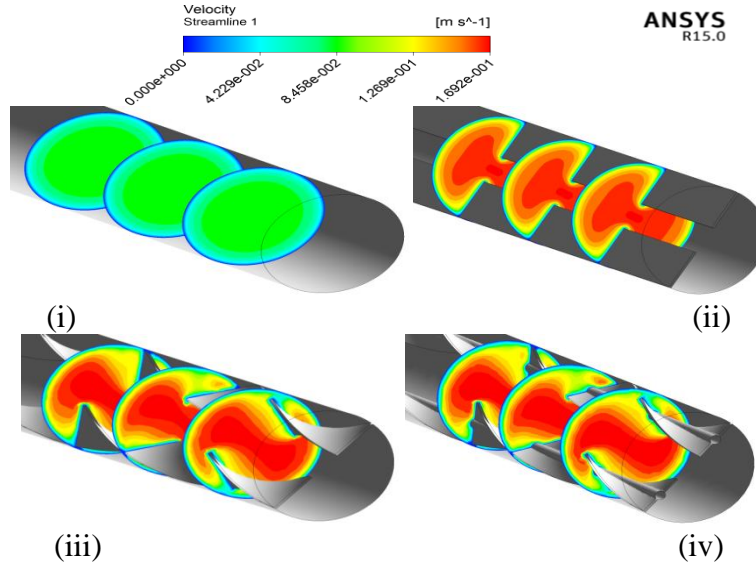


Fig. 6. Velocity contours and streamlines for; (i)PT, (ii)TDPT, (iii)TDPTT and (iv)TDHSTT.

As seen in the Fig. (6 [frame ii]), The velocity increase by 41.7768% for TDPT higher than plain tube (PT). That occur due to the decrease in hydraulic diameter of fluid flow cross sectional area by act of tape geometry which increase mean velocity at constant Reynolds number to satisfy equation of continuity (the rate of mass enters a system is equal to the rate of mass leaves the system).

For TDPTT and TDHSTT, the velocity increased by 0.1526% and 0.2184% higher than TDPT, this slightly increase occur due to swirl motion generated in the boundary flow region and turbulence fluctuations produced by these geometries. In addition to, these tapes break boundary layer

propagation and mix fluid flow layers between near wall region and core region lead to appears of high velocity region in tube core and increase fluid velocity at boundary region, that lead to an increase even if it an noticeable in average velocity of fluid flow.

Longitudinal vortices in flow fields are shown in Fig. (7) which illustrated the rotational flow zone only, it has been found that the vortices generated in the flow by act of the dual twisted tape and the dual helical screw twisted tape are approximately the same with small higher vorticity magnitude resulted in using TDHSTT up to 1.63% over the flow in case of TDPTT.

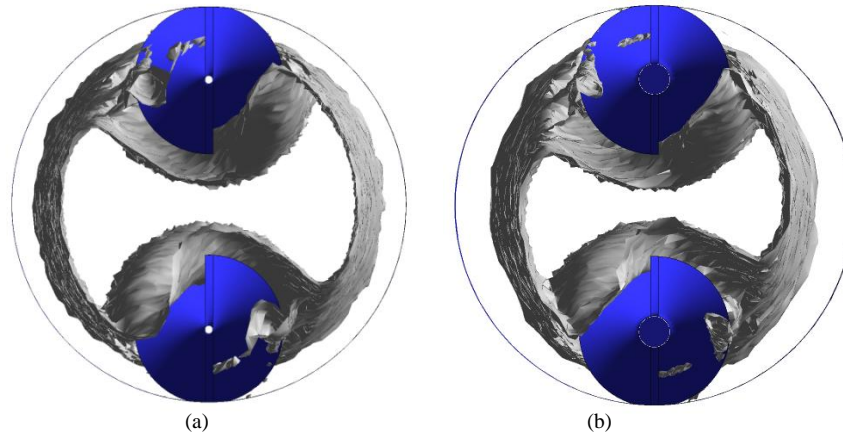


Fig. 7. Longitudinal vortices for tube fitted with; (a) dual plain twisted tape, TDPTT, (b) dual helical screw twisted tapes, TDHSTT.

The velocities of the nanofluid are approximately the same to those of water under the previously defined nanoparticles volume fraction, which show up that nanofluid will not require undesirable increase in pumping power.

### 6.1.2 Pressure Drop Contours

A pressure drop will be occur whenever fluid flow. The main factors that affects pressure drop are fluid viscosity and flow velocity. Pressure contours are illustrated in Fig. (8) for the three considered models at Reynolds number range of 7,500 for *water flow* and on longitudinal revolution surface along the axial direction.

In the case of TDPT, Fig.(8 [frame a]), pressure drop is 103.3895% more than in PT due to the fact that inserts as additional surfaces increase shear forces act on fluid flow which proportional vary with the pressure drop.

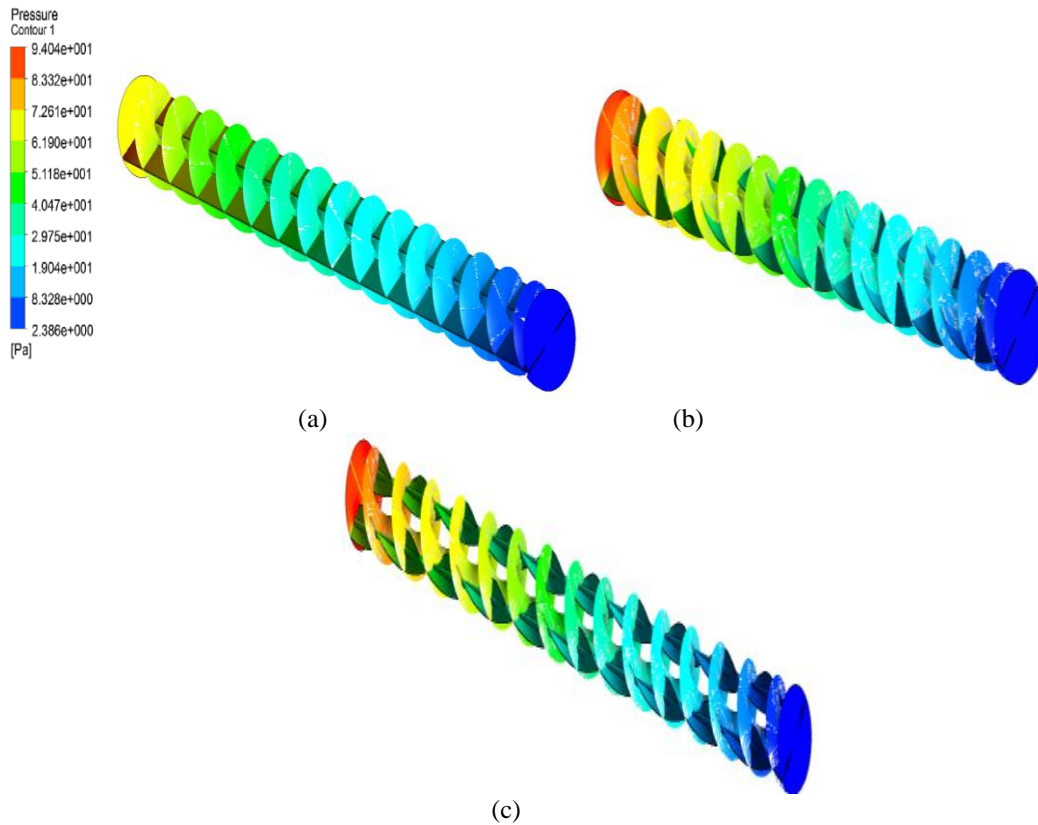


Fig. 8. Pressure contours for a longitudinal revolution surface along the computational domains; (a) TDPT, (b)TDPTT and (c)TDHSTT.

The pressure drop in TDPTT and TDHSTT are 28.715% and 30.8% larger than TDPT, respectively.

That due to secondary motion produced by each one of them, where the vortex motion achieved by twisted tapes and helical screw twisted tapes effect on velocity proportionally as explained previously, where resulted velocity gradient change in harmony with shear forces acting on fluid flow which give rise to pressure drop.

Pressure drop increase slightly by using nanofluid at 0.1% volume fraction, as shown in Fig. (9), the numerical results

shown an increase between water and nanofluid up to +7% for the same model investigated.

However, experimental results for pressure match well with those predicted numerically with a deviation range of  $\pm 5.06\%$ . It's obvious from Fig. (9) that pressure drop of water and for nanofluid increase with increasing Reynolds number, the small increase in pressure drop of nanofluid than water illustrate that using nanofluids with higher particle volume fraction may cause small penalty in pressure drop.



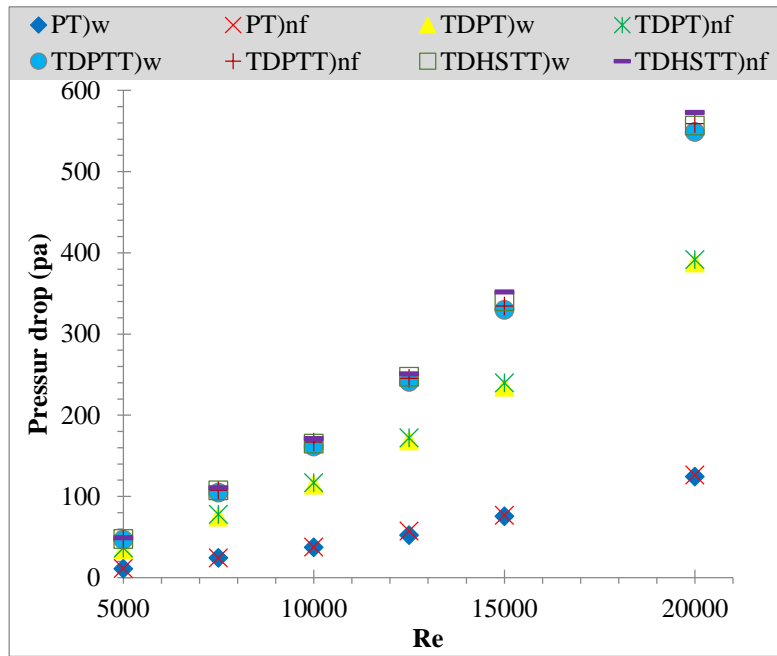


Fig. 9. Comparison of pressure drop obtained from water (w) and that from TiO<sub>2</sub>/water nanofluid (nf) for different inserts and Reynolds numbers.

### 6.1.3 Friction Factor

Velocity variation, pressure drop and other flow variables have an impact on the friction factor, as in eq. (13) previously. The models examined computationally and experimentally and results are discussed below.

The experimental results match the results obtained from correlations (14-16) with a deviation up to 8.69%, the results of validation are shown in Fig. (10). Measured friction factors agree well with the determined values from correlations of validation.

As Reynolds number increase, the friction factor decrease. This is because Reynolds number increases the momentum overcomes the viscous forces of fluid and consequently lowers the shear between the fluid and the tube wall.

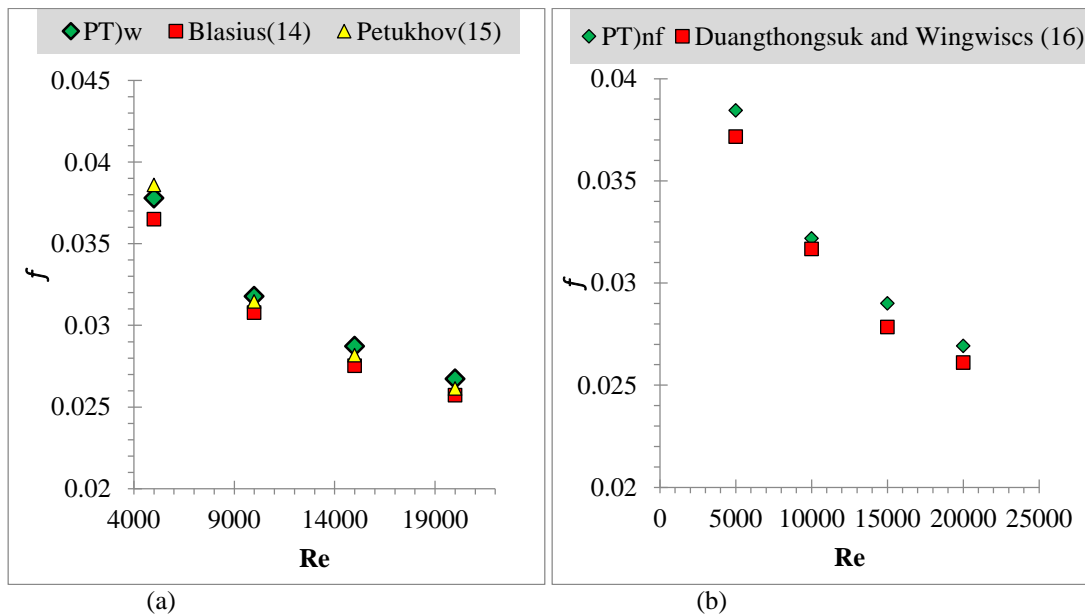


Fig. 10. Validation of measured friction factors experimentally and those calculated from; (a) equations (14) and (15) for water flow (w) in PT, (b) equations (16) for nanofluid flow (nf) in PT.

The variation of the friction factor with Reynolds number for the tubes with different models of inserts with flows of water and nanofluid are compared in Fig. (11). the friction factors of the nanofluids are slightly higher than those of the water. The tube equipped with dual plain tapes inserts (TDPT) when water flow has friction factor of 5.12 to 12.13% higher than plain tube. This is attributed to the additional surfaces provided by mechanism of inserts enhancement, for the same case, friction factor increases by 1.38-2.458% with using nanofluid.

The additional dissipation of pressure of the fluid caused by the fluid disturbance due to secondary flow produced by swirl generators result in an increase in pressure drop and frictional losses. Therefore, for water flow, the friction factors of TDPTT and TDHSTT are +9.57 to 15.358% and +11.41 to 17.349% higher than that in (PT).

for  $\text{TiO}_2/\text{Water}$  flow, the friction factors of TDPTT and TDHSTT are 9.92 to 15.863% and 11.82 to 17.88% higher than that in (PT).

These results by comparing with pressure drop results, illustrated in section (6.1.2), shown the effect of pressure drop on friction factor where the model has higher pressure drop will show higher friction factor as in the case of tube fitted with dual helical screw twisted tapes (TDHSTT). As from (13), friction factor represent ratio of static pressure difference over dynamic pressure where dynamic pressure in term of inlet velocity differ between models due to the differences between flow cross sectional areas and type of motion.

Numerical results predicted for friction factor shows the same behavior as experimental once where differentiations between these two obtained results were within  $\pm 5.04\%$  deviation range which can be considered as an acceptable limit.

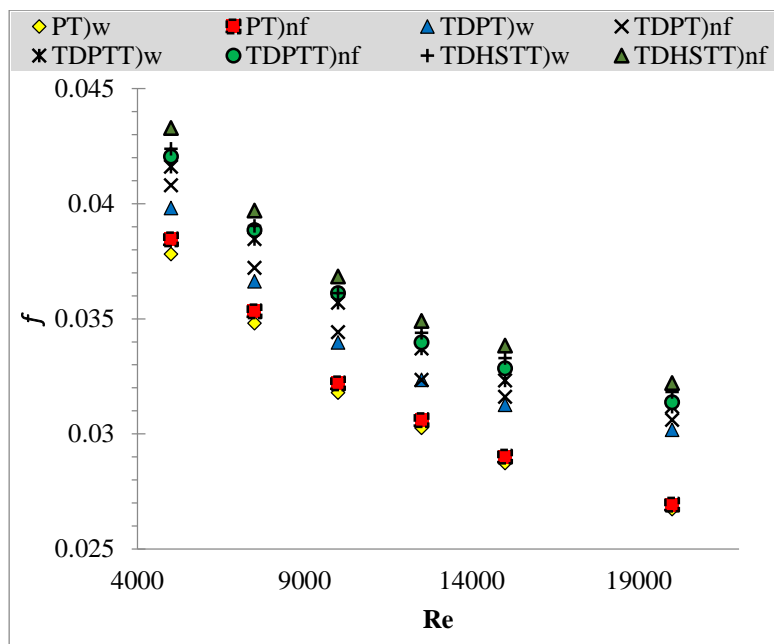


Fig. 11. Variation of experimental results for friction factor with Reynolds number for plain tube and tube induced with different models of inserts for both water flow (w) and nanofluid flow (nf).

## 6.2 Heat Transfer Enhancement

The enhancement in heat transfer rate was presented in term of Nusselt number, as shown in eqs. (11) and (12) previously, it is influenced by velocity variation, friction factor, nanoparticles volume fraction, twisted tape dimensions and other parameters. The models examined experimentally in the turbulent Reynolds range of (5,000-20,000).

The experimental results match those results obtained from correlations (11-12) with a deviation of 2.6179% - 6.13%; the results of validations are shown in Figs. (12-13).

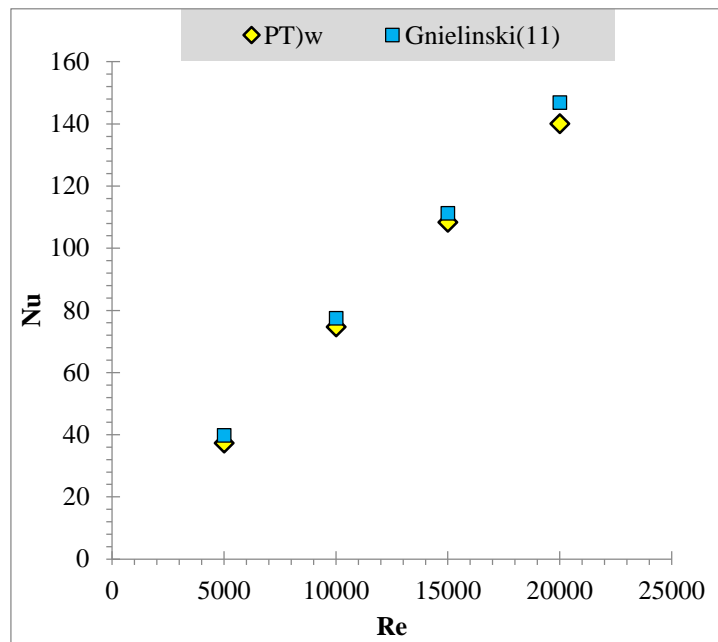


Fig. 12. Validation of experimental results for Nusselt number to the plain tube with Gnielinski correlation for water flow.

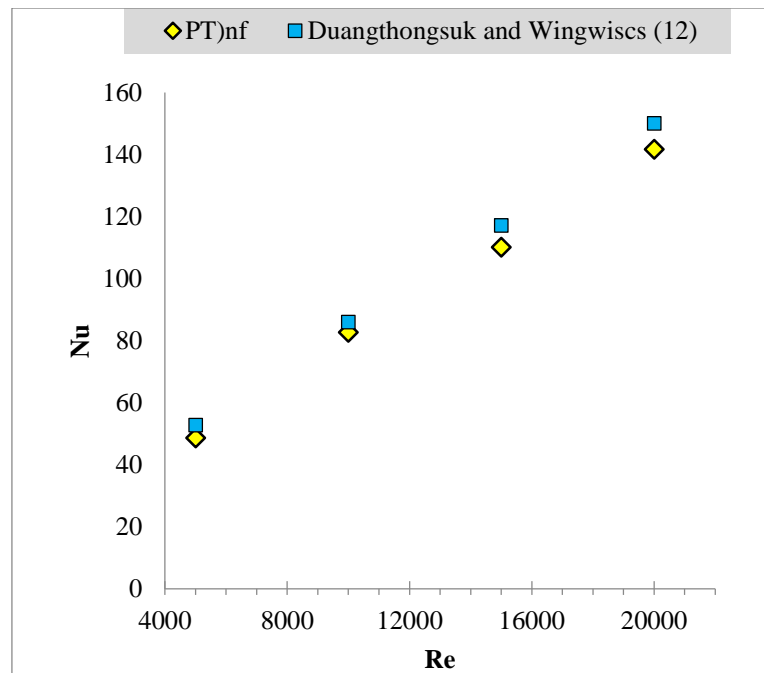


Fig. 13. Validation of experimental results for Nusselt number to the plain tube with Duangthongsuk and Wingwisets correlation for nanofluid flow.

The variation of Nusselt number with Reynolds number for the tubes with strips, twisted tapes and helical screw twisted tapes inserts are compared in Fig. (14) for both nanofluid and base fluid. It can generally be noticed that the Nusselt number increases with the increase of Reynolds number.

For water flow, the TDPT has Nusselt numbers of 42.7 to 55.72% higher than plain tube, this enhancement in heat transfer rate return to the act of strips that blockage flow and break thermal boundary layer developing which lead the temperature distribution to uniformity that resulted in higher temperature gradient and enhance heat transfer coefficient.

Nusselt numbers of TDPTT and TDHSTT are 47.82 to 72.58% and 52.242 to 75% higher than that in case of plain tube (PT). It's obvious that Nusselt number increases due to vortex motion higher than linear motion, where the swirl (vortex) motion act on increase turbulence intensity and disturb the uniformity at boundary flow region which can be recognized as the key factor of heat transfer enhancement.

For  $\text{TiO}_2/\text{water}$  nanofluid flow, PT, TDPT, TDPTT and TDHSTT have Nusselt numbers of 1.27 to 30.43%, 46.07 to 64%, 49.5 to 76.38% and 55.3 to 82.2%, respectively, higher than that observe for (PT) with water flow. This behaviour due to the fact that nanoparticles which dissolved in the water increase the thermal conductivity that leads to an increase in heat transfer rate.

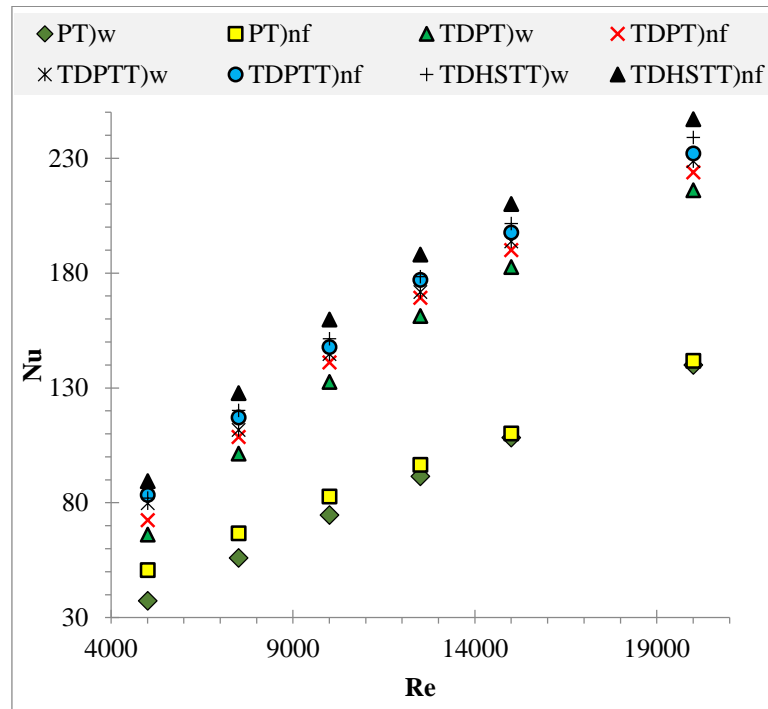


Fig. 14. Variation of Nusselt number with Reynolds number for plain tube and tubes induced with different models of tapes inserts.

## 7. CONCLUSIONS

The thermo-hydraulic characteristics of tubes induced with dual strips, dual plain twisted tapes and dual helical screw twisted tapes inserts using water and nanofluid were numerically and experimentally carried out. The investigation was achieved under turbulent flow condition for a Reynolds number of a range within 5,000-20,000. The findings are presented below;

- i- The induced tubes were experimentally and numerically investigated for turbulent regime of water and ( $\text{TiO}_2/\text{water}$ ) nanofluid flows for each mentioned designs and was found that the tube fitted with dual helical screw twisted tapes (TDHSTT) gave the best heat transfer rate enhancement. The Nusselt number of

this model was up to 82.2% for nanofluid flow and 75% for water flow higher than in plain tube (PT) with water flow.

- ii- As Reynolds number increase, higher Nusselt number obtained from induced tube than plain tube.
- iii- The pressure drop and friction factor increase significantly by using inserts and slightly by nanofluid.
- iv- Using nanofluids with inserts lead to more heat transfer augmentation than use each one individually.
- v- Using inserts need to increase fluid pumping power due to high pressure drop produced. When using nanofluid without inserts, pumping power not affected.
- vi- Pressure drop increase as Reynolds number increase while friction factor decrease with Reynolds number increases.

**Abbreviations**

$D$	Tube diameter (mm)
$f$	Friction factor
$I$	Turbulence intensity
$K$	Thermal conductivity (W/m.K)
$L$	Tube length (mm)
$Nu$	Nusselt number
$\Delta p$	Pressure drop (Pa)
$Pr$	Prandtl number
$\bar{q}$	Heat flux (W/m <sup>2</sup> )
$Re$	Reynolds number
$V$	Mean velocity (m/s)
$w$	Tape width (mm)
$y$	Tape pitch 180° (mm)
$\delta$	Tape thickness (mm)
$\nu$	Kinematic viscosity (m <sup>2</sup> /s)
$\varphi$	Nanoparticles volume fraction (%)
$\rho$	Fluid density (kg/m <sup>3</sup> )
$\mu$	Fluid dynamic viscosity (kg/m.s)
$c_p$	Fluid specific heat (J/kg.K)

**Subscripts**

b	Bulk
h	Hydraulic
in	Inlet
nf	Nanofluid
s	Surface
w	water

**ACRONYMS**

PT	Plain tube
TDPT	Tube with dual plain tapes
TDPTT	Tube with dual plain twisted tapes
TDHSTT	Tube with dual helical screw twisted tapes

**8.****REFERENCES**

- [1] Behabadi, M. A., Hejazi, V. and Afshari, A., (2010). "Experimental Investigation of Twisted Tape Inserts Performance on Condensation Heat Transfer Enhancement and Pressure Drop", International Communications in Heat and Mass Transfer, Vol. 37, pp. 1376–1387.
- [2] Bergles, A.E. and Manglik, R.M. (1993). "Heat Transfer and Pressure Drop Correlations for Twisted Tape Inserts in Isothermal Tube: Part II-Transition and Turbulent Flows", Transaction of ASME Journal of Heat Transfer, Vol. 115, pp. 890-896.
- [3] Sundar, L. S. and Sharma, K.V., (2010), "Turbulent Heat Transfer and Friction Factor of Al<sub>2</sub>O<sub>3</sub> Nanofluid in Circular Tube with Twisted Tape Inserts", International Journal of Heat and Mass Transfer, Vol. 53, pp. 1409–1416.
- [4] He, Y., Men, Y., Zhao, Y., Lu, H., Ding, Y., (2009). "Numerical Investigation into The Convective Heat Transfer of TiO<sub>2</sub> nanofluids Flowing Through a Straight Tube under the Laminar Flow Conditions". Applied Thermal Engineering, Vol. 29, pp. 1965-1972.
- [5] Hu, N. H. and Chang, Y. P., (1973), "Optimization of Finned Tubes for Heat Transfer in Laminar Flow," ASME Journal of Heat Transfer, Vol. 95, No. 3, pp. 332-338.
- [6] Kelkar, K. M. and Patankar, S. V., (1990), "Numerical Prediction of Fluid Flow and Heat Transfer in a Circular Tube with Longitudinal Fins Interrupted in Stream Wise Direction", ASME Journal of Heat Transfer, Vol. 112 No.2, pp. 342-348.
- [7] Pourrajabi, M., Nezhad, A.R., Pourrajabi, M.R., (2013). "Numerical Study of Turbulent Flow and Heat Transfer of a Nanofluid in a Circular Tube with Twisted Tape Insert", International Symposium on Advances in Science and Technology, 7<sup>th</sup> SASTech, Iran.
- [8] Said, Z., Saidur, R., Hepbasli, A., Rahim, N.A., (2014). "New Thermophysical Properties of Water Based TiO<sub>2</sub> nanofluid- The Hysteresis Phenomenon Revisited ", International Communications in Heat and Mass Transfer, Vol. 58, pp. 85-95.
- [9] Maddah, H., Farokhi, M., Aghayari, R., Jahanizadeh, S., Ashtary, K., (2014), "Effect of Twisted-Tape Turbulator and Nanofluid on Heat Transfer in a Double Pipe Heat Exchanger", Journal of Engineering, Hindawi publishing Co., Vol. 2014, A.I.D. 920970.
- [10] Eiamsa-ard, S., Safikhani, H., (2015), "Multi-Objective Optimization of TiO<sub>2</sub>-Water Nanofluid Flow in Tubes Fitted with Multiple Twisted Tape Inserts in Different Arrangement", Trans. Phenom. Nano Micro Scale, 3(2), pp. 89-99.
- [11] Sandesh S. C. and Sahu, S. K., (2013), "Comparative Study on Heat Transfer Enhancement of Low Volume Concentration of Al<sub>2</sub>O<sub>3</sub>-Water and Carbon Nanotube-Water Nanofluids in Laminar Regime Using Helical Screw Tape Inserts", Journal of Nanotechnology in Engineering and Medicine, Vol.4.
- [12] Chun, B. H., Kang, H. U, and Kim, S. H., (2008), "Effect of Alumina Nanoparticles in the Fluid on Heat Transfer in Double-pipe Heat Exchanger System," Korean Journal of Chemical Engineering, Vol. 25, No. 5, pp. 966–971.
- [13] Duangthongsuk, W. and Wongwises, S., (2008), "Effect of Thermophysical Properties Models on the Predicting of the Convective Heat Transfer Coefficient for Low Concentration Nanofluid", International Communications in Heat and Mass Transfer, Vol. 35, No.10, pp. 1320–1326.
- [14] Santra, A. K., Sen, S., and Chakraborty, N., (2009), "Study of Heat Transfer due to Laminar Flow of Copper-Water Nanofluid through Two Isothermally Heated Parallel Plates", International Journal of Thermal Sciences, Vol. 48, No. 2, pp. 391–400.
- [15] Namburu, P. K., Das, D. K., Tanguturi, K. M., and Vajjha, R. S., (2009), "Numerical Study of Turbulent Flow and Heat Transfer Characteristics of Nanofluids Considering Variable Properties", International Journal of Thermal Sciences, Vol. 48, No. 2, pp. 290-302.
- [16] Gherasim, I., Roy, G., Nguyen, C. T., and Vo-Ngoc, D., (2009), "Experimental Investigation of Nanofluids in Confined Radial Flows", International Journal of Thermal Sciences, Vol. 48, No. 8, pp. 1486–1493.

- [17] Pak, B. C. and Cho, Y. I., (1998), "Hydrodynamic and Heat Transfer Study of Dispersed Fluids with Submicron Metallic Oxide Particles," *Experimental Heat Transfer*, Vol. 11, No. 2, pp. 151–170.
- [18] Reddy, M., Rao, V.V., Reddy, B., Sarada, S. N., Ramesh, L., (2012), "Thermal Conductivity Measurements of Ethylene Glycol Water based  $TiO_2$  nanofluids", *Nanosci. Nanotechnology. Lett.* 4, pp. 105–109.
- [19] Incropera, F.P and DeWitt, P.D., Bergman, T.L. and Lavine, A.S. (2006), "Fundamentals of Heat and Mass Transfer", John-Wiley & Sons.
- [20] Chiu, Y.W. and Jang, J.Y. (2009), "3D Numerical and Experimental Analysis for Thermal-Hydraulic Characteristics of Air Flow Inside a Circular Tube with Different Tube Inserts", *Applied Thermal Engineering* 29 ,pp. 250–258.
- [21] Chakole, M.M., and Sali, N.V. (2015). " Experimental Investigation of Thermal Characteristics with Multiple Twisted Tape Inserts in Tubular Heat Exchanger", *International Journal of Advance Research In Science And Engineering*, Vol. 4, Issue 04.